

1-1-2009

Femtosecond two-photon absorption measurements based on the accumulative photothermal effect and the Rayleigh interferometer

Luis Rodriquez
University of Central Florida

Hyo-Yang Ahn
University of Central Florida

Kevin D. Belfield
University of Central Florida

Find similar works at: <https://stars.library.ucf.edu/facultybib2000>
University of Central Florida Libraries <http://library.ucf.edu>

This Article is brought to you for free and open access by the Faculty Bibliography at STARS. It has been accepted for inclusion in Faculty Bibliography 2000s by an authorized administrator of STARS. For more information, please contact STARS@ucf.edu.

Recommended Citation

Rodriquez, Luis; Ahn, Hyo-Yang; and Belfield, Kevin D., "Femtosecond two-photon absorption measurements based on the accumulative photothermal effect and the Rayleigh interferometer" (2009). *Faculty Bibliography 2000s*. 2064.
<https://stars.library.ucf.edu/facultybib2000/2064>

Femtosecond two-photon absorption measurements based on the accumulative photo-thermal effect and the Rayleigh interferometer

Luis Rodriguez,^{1, 2, 3} Hyo-Yang Ahn,¹
and Kevin D. Belfield^{1, 2,*}

¹Department of Chemistry, The College of Optics and Photonics, University of Central Florida, P.O. Box 162366, Orlando, Florida 32816-2366, USA

²CREOL, The College of Optics and Photonics, University of Central Florida, P.O. Box 162366, Orlando, Florida 32816-2366, USA

³Departamento de Física, Universidad Simón Bolívar, Caracas 1080-A, AP 89000, Venezuela
[*belfield@mail.ucf.edu](mailto:belfield@mail.ucf.edu)

Abstract: A rapid, straightforward method for measuring the two-photon absorption cross sections in liquid samples based on both the accumulative photo-thermal effect and the Rayleigh interferometry is described and demonstrated. This technique combines the sensitivity of the thermal lens approach and the accuracy of interferometry techniques. Focusing a high repetition rate laser beam in the sample, generating a localized change in its refractive index, induces the photo-thermal phase shift. By recording and processing two interference patterns, this technique allows the rapid estimation of the two-photon absorption cross section of the sample. Significantly, the experimental results demonstrate that this new method can be used with both fluorescent and non-fluorescent samples.

©2009 Optical Society of America

OCIS codes: (190.0190) Nonlinear optics; (190.4870) Photothermal effects; (260.3160) Interference; (300.6410) Spectroscopy, multiphoton; (300.6280) Spectroscopy, fluorescence and luminescence.

References and links

1. P. Sengupta, J. Balaji, S. Banerjee, R. Philip, G. R. Kumar, and S. Maiti, "Sensitive measurement of absolute two-photon absorption cross sections," *J. Chem. Phys.* **112**(21), 9201–9205 (2000).
2. M. Sheik-Bahae, A. A. Said, T.-H. Wei, D. J. Hagan, and E. W. Van Stryland, "Sensitive Measurement of Optical Nonlinearities Using a Single Beam," *IEEE J. Quantum Electron.* **26**(4), 760–769 (1990).
3. A. Dragomir, J. G. McInerney, D. N. Nikogosyan, and A. A. Ruth, "Two-photon absorption coefficients of several liquids at 264 nm," *IEEE J. Quantum Electron.* **38**(1), 31–36 (2002).
4. C. Xu, and W. Webb, "Measurements of two-photon excitation cross section of molecular fluorophores with data from 690 to 1050nm," *J. Opt. Soc. Am. B* **13**(3), 481–491 (1996).
5. P. Kaatz, and D. P. Shelton, "Two-photon fluorescence cross-section measurements calibrated with hyper-Rayleigh scattering," *J. Opt. Soc. Am. B* **16**(6), 998–1006 (1999).
6. N. S. Makarov, M. Drobizhev, and A. Rebane, "Two-photon absorption standards in the 550-1600 nm excitation wavelength range," *Opt. Express* **16**(6), 4029–4047 (2008).
7. A. Marcano O., "K. Williams, N. Melikechi, "Measurement of two-photon absorption using the photo-thermal lens effect," *Opt. Commun.* **281**, 2598–2604 (2008).
8. N. J. Dovichi, and J. M. Harris, "Laser Induced Thermal Lens Effect for Calorimetric Trace Analysis," *Anal. Chem.* **51**(6), 728–731 (1979).
9. A. J. Twarowski, and D. S. Kliger, "Multiphoton absorption spectra using thermal bloomingII. Two-photon spectrum of benzene," *Chem. Phys.* **20**(2), 259–264 (1977).
10. M. Falconieri, "Thermo-optical effects in Z-scan measurements using high-repetition-rate lasers," *J. Opt. A, Pure Appl. Opt.* **1**(6), 662–667 (1999).
11. J. Stone, "Measurements of the Absorption of Light in Low-Loss Liquids," *J. Opt. Soc. Am.* **62**(3), 327–333 (1972).
12. L. Rodriguez, C. Simos, M. Sylla, A. Marcano, and X. Nguyenphu, "New holographic technique for third-order optical properties measurement," *Opt. Commun.* **247**(4-6), 453–460 (2005).
13. M. Born, and E. Wolf, *Principles of Optics*, (Cambridge University Press, 1999).
14. M. Falconieri, and G. Salvetti, "Simultaneous measurement of pure-optical and thermo-optical nonlinearities induced by high-repetition-rate, femtosecond laser pulses: application to CS₂," *Appl. Phys. B* **69**(2), 133–136 (1999).

15. S. J. Sheldon, L. V. Knight, and J. M. Thorne, "Laser-induced thermal lens effect: a new theoretical model," *Appl. Opt.* **21**(9), 1663–1669 (1982).
 16. R. A. Ganeev, A. I. Rysanyansky, M. Baba, M. Suzuki, N. Ishizawa, M. Turu, S. Sakakibara, and H. Kuroda, "Nonlinear refraction in CS₂," *Appl. Phys. B* **78**(3-4), 433–438 (2004).
 17. S. Couris, M. Renard, O. Faucher, B. Lavorel, R. Chaux, E. Koudoumas, and X. Michaut, "An experimental investigation of the nonlinear refractive index (n_2) of carbon disulfide and toluene by spectral shearing interferometry and z-scan techniques," *Chem. Phys. Lett.* **369**(3-4), 318–324 (2003).
 18. C. Gorecki, "Interferogram analysis using a Fourier transform method for automatic 3D surface measurement," *Pure Appl. Opt.* **1**(2), 103–110 (1992).
 19. M. A. Albota, C. Xu, and W. W. Webb, "Two-photon fluorescence excitation cross sections of biomolecular probes from 690 to 960 nm," *Appl. Opt.* **37**(31), 7352–7356 (1998).
-

1. Introduction

Two types of methods are frequently used to measure the two-photon absorption (2PA) coefficients (β). In one method, low sensitivity nonlinear transmission techniques (e.g., z-scan) [1–3], applicable for both non-fluorescent and fluorescent samples, measure the transmitted light through the sample when a strong laser beam is focused into the medium. Due to its low sensitivity, these methods require high concentrations of the sample and high intensity levels, possibly leading to sample decomposition. The other method is fluorescence-based [4–6], directly collecting the light emitted from the sample when a 2PA process is induced. Although this method is more sensitive, it is limited to fluorescent samples and to the frequently high uncertainties in the measurements due to reabsorption and other effects. Thermal lensing (TL) spectrometry is an analytical method used for measurement with high sensitivity of thermo-optical properties in neat liquids and solutions [7,8]. Twarowski and Kliger [9] developed a technique to measure the 2PA cross section in the nanosecond time regimen using the TL effect. This technique was later adapted by Falconieri [10], employing femtosecond laser pulses at high repetition rate (HRR), to measure nonlinear optical properties in standard solvents.

When a single laser pulse passes through the sample, in a typical TL experiment, part of the absorbed energy is converted into heat, inducing a localized temperature rise in the sample. The duration time of this temperature rise depends on the characteristic relaxation time (t_c , see below) of the thermal lens [9]. If the time period between laser pulses is greater than the characteristic time the TL vanishes after the laser pulse; allowing the sample to return to the initial temperature. Otherwise, if the time period is less than the characteristic time, the sample does not return to its initial temperature, and, as consequence, accumulative heating is generated in the sample. This heating can be produced by absorption of one or two photons by the sample, generating a distribution of temperatures that consequently produces a change in the spatial distribution of the refractive index. The induced TL distorts the wave front of the laser beam at the exit plane of the sample. By measuring this distortion, the thermo-optical parameters or nonlinear absorbance of the sample can be estimated.

Despite its intrinsic sensitivity and experimental simplicity, TL techniques require accurate data for the sample position, including the pump beam waist, Rayleigh range of the pump beam, degree of the mode mismatching of the probe-pump beams, and characteristic thermal time constant in order to estimate β . Beside TL, interferometric methods provide accurate measurements of linear or nonlinear optical properties [11,12] without having to know all of the experimental parameters.

We demonstrate an approach that combines the sensitivity of the TL technique and the accuracy of interferometric methods. This approach is based on a modified Rayleigh interferometer [13] and the accumulative photo-thermal effect induced by a HRR laser. The Rayleigh interferometer is frequently used to determine the refractive indices of gases with high accuracy, due to its intrinsic sensitivity to measure small refractive index changes. The accumulative TL technique has been observed in closed-aperture z-scan experiments, influencing significantly the determination of the nonlinear refractive index [10,14]. The technique consists of measuring β from the sample under study, accomplished by inducing an accumulative TL and measuring its effect on the phase shift of an interference pattern. The

technique has the following advantages: a) a simple experimental setup, b) total absence of mechanical movements of the sample during the measurement, c) fast recording and processing of the experimental data, and d) good sensitivity in the measurement of small phase shifts. However, our method has limitations, among them: a) several parameters are necessary to estimate β ; b) it is only applicable to samples with negligible linear absorbance. Herein, we report using a stationary TL generated by an HRR laser in order to measure nonlinear absorption (specifically 2PA) coefficients in fluorescent or non-fluorescent media and both neat liquids and relatively dilute solutions.

2. Theoretical considerations

Figure 1 illustrates the schematic diagram of the interferometer used in our approach in order to measure small changes of refractive index in liquid samples induced by an accumulative photo-thermal effect. In the classical Rayleigh interferometer, two beams pass through two samples of the same path length containing gases whose refractive indices are to be compared. In our approach, both beams pass through the same sample and the refractive index to be compared is induced by a localized TL in the sample. Beams <1>, <2> and <3> are delivered by a HRR laser system and the transparent optical medium (sample), characterized by nonlinear absorption coefficient β and negligible linear absorbance, is placed in the optical axis of these beams. It is assumed that beams <1> and <2> have identical phases, intensities, and diameters. After they pass through the sample, a positive lens focuses them together on a focal plane, producing a parallel interference pattern. Since the intensities of these two beams are weak, the interferogram only contains information about the linear refractive index of the sample. When a strong pump beam <3> is impinged in the sample, an accumulative photo-thermal effect or TL is localized around the optical axis of beam <3>. A small angle between beams <1> and <3> localizes the TL in the center of the probe beam <1>, and, therefore, its phase is homogeneously shifted with respect to the phase of the reference beam <2>. As a consequence of this induced TL, the phase in the interference pattern changes, allowing determination of the phase shift and calculation of the 2PA coefficient of the sample.

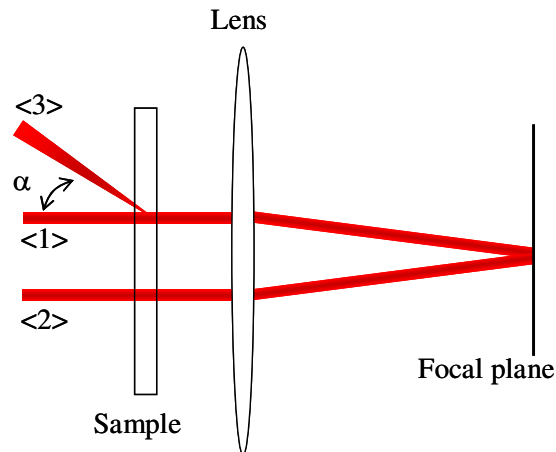


Fig. 1. Schematic diagram of the thermal lens method based on a Rayleigh interferometer.

We have based our approach on a theoretical model developed in [15] and adapted it for the case of the TL induced by absorption of two photons when light from a HRR laser is applied to the sample. In this case, the heat source, radial energy flow into the sample in a unit of volume and a unit of time, can be described by the following equation:

$$Q(r) = \beta I(r)^2, \quad (1)$$

where $I(r)$ is the incident intensity of the beam in the sample. Due to the HHR of the laser, we considered an average intensity described by $I(r) = 2P \exp(-2r^2/w^2) / \pi w^2$, where w is the radius of the beam in the sample and P is the average incident power. By solving the heat conduction equation [15] with the heat source (Eq. (1)), we obtained an expression for the temperature distribution induced by an accumulative 2PA photo-thermal effect:

$$\Delta T(r, t) = \left(\frac{\beta P^2}{\pi^2 w^2 \kappa} \right) \frac{1}{t_c} \int_0^t \frac{1}{1 + 4t'/t_c} \exp\left(\frac{-4r^2/w^2}{1 + 4t'/t_c} \right) dt', \quad (2)$$

where κ is the thermal conductivity of the sample and $t_c = w^2/4D$ is the characteristic relaxation time of the thermal lensing, while D is the thermal diffusivity of the medium. Note that if the linear absorbance of the sample cannot be neglected, an expression equivalent to the Eq. (8) of reference 15 has to be added to Eq. (2) in order to calculate the correct temperature rise. In our calculations, we assume negligible single-photon absorbance at the excitation wavelength. In this case, the temperature distribution given by Eq. (2) induces an additional phase in the wavefront of a probe beam $\langle 1 \rangle$. This photo-thermal phase shift is given by: $\phi = (2\pi L/\lambda) \Delta n$, where L is the sample path length, λ the wavelength of the laser, and $\Delta n = (dn/dT) \Delta T$ being (dn/dT) the thermo-optic parameter. By writing the exponential integral in Eq. (2) as a power series, the 2PA photo-thermal phase shift is described by Eq. (3):

$$\phi(r, t) = \frac{\beta L P^2}{2\pi w^2 \lambda \kappa} \left(\frac{dn}{dT} \right) \left\{ \ln(1 + 4t/t_c) + \sum_{i=1}^{\infty} \frac{(-4r^2/w^2)^i}{i!} \left[1 - \left(\frac{1}{1 + 4t/t_c} \right)^i \right] \right\}. \quad (3)$$

In this expression, we assume that the nonlinear phase shift ($2\pi L n_2 I_0 / \lambda$, where n_2 is the nonlinear refractive index) is much smaller than the photo-thermal phase when low incident power is used. In order to evaluate the magnitude of the phase shift induced by a 2PA process, the phase variation around the optical axis of the pump beam is considered. This is done by first calculating the phase difference between the center and the extreme ($r = w$) of the excitation Gaussian beam ($\Delta\phi(t) = \phi(w, t) - \phi(0, t)$), followed by evaluation of the phase difference when the steady state is reached ($t \rightarrow \infty$). Under these conditions the Eq. (3) can be rewritten as:

$$\Delta\phi = \Delta\phi(\infty) - \Delta\phi(0) \approx 1.32 \frac{\beta L P^2}{2\pi w^2 \lambda \kappa} \left(\frac{dn}{dT} \right). \quad (4)$$

Although this expression is obtained with the assumption that the stationary thermal lens is a perfect lens with no aberration, its accuracy is suitable for a small phase shift ($\Delta\phi < 1$) measured on-axis pump beam. This is because experimental variables such as reflections of the cell walls, optimal position of the sample, and experimental setup geometry of pump-probe beams are not required. If the sample in question is fluorescent, Eq. (4) must be multiplied by the quantity $(1 - \Phi \lambda / 2 \langle \lambda_e \rangle)$ because the two-photon up-converted fluorescence occurs in addition to the heat source. This equation is deduced by considering the number of photons absorbed and emitted per second when the 2PA process is induced. The ratio $\lambda / 2 \langle \lambda_e \rangle$ takes account the Stokes shift. The parameter Φ is the quantum yield, and $\langle \lambda_e \rangle = \int E(\lambda) d\lambda / \int [E(\lambda) / \lambda] d\lambda$ is the average wavelength of the emitted light, where $E(\lambda)$ is the two-photon up-converted fluorescence spectrum of the sample. The factor $\frac{1}{2}$ is due to two photons being necessary to produce one fluorescence process.

The induced photo-thermal phase shift was measured with the modified Rayleigh interferometer described above. We considered that the dimension of the thermal lens is smaller than the separation between beams $\langle 1 \rangle$ and $\langle 2 \rangle$. Therefore, only the complex amplitude of the electric field of probe beam $\langle 1 \rangle$ is locally altered by the phase shift; while the phase of probe beam $\langle 2 \rangle$ remained constant, and was used as the reference beam carrying only the linear phase difference in the interferogram. At the focal plane of the lens, the intensity distribution of the interference pattern in the x -direction is given by:

$$i(x, y) = a(x, y) + b(x, y) \cos(2\pi x / \Delta x + \phi(x, y)), \quad (5)$$

where $a(x, y)$ and $b(x, y)$ are functions related with the intensity distributions of the probe-reference beams, and pattern fringe visibility. The parameter x is the distance from the center of the pattern, Δx is the fringe spacing, and y is the perpendicular coordinate axis. In Eq. (5), we assumed that $\phi(x, y)$ produces a small phase shift in the interference pattern while the fringe spacing remained constant.

The phase $\phi(x, y)$ can be extracted from Eq. (5) by taking the Fourier transform in two dimensions for the interference pattern [12]:

$$I(X, Y) = A(X, Y) + \left[FT(\exp(-j\phi(x, y))) * B(X, Y) \right] \otimes \delta(X - \Delta X, Y) \\ + \left[FT(\exp(j\phi(x, y))) \otimes B(X, Y) \right] \otimes \delta(X + \Delta X, Y), \quad (6)$$

where FT represents the Fourier transform, \otimes the convolution operator, X and Y the spatial frequency variables, and $\delta(X \pm \Delta X, Y)$ the Dirac's delta function. The last two terms in Eq. (6) are two Dirac's distributions placed in $\pm \Delta X$ around the low spatial frequency $A(X, Y)$. By using a band pass filter, it was possible to extract one of these Dirac's delta. Taking the inverse 2D-FT of the extracted Dirac's distribution, we obtained the following complex function:

$$g(x, y) = b(x, y) \exp(-j\phi(x, y)). \quad (7)$$

In this equation, we needed to eliminate any possible influence of the linear phase shift in the function $b(x, y)$. This was accomplished by evaluating the interferogram (Eq. (5)) in the absence of the thermal lens ($\phi(x, y) = 0$), and performing the same Fourier treatment previously described. Taking into account the complex functions $g(x, y)$ and $b(x, y)$ we obtained the nonlinear transfer function $h(x, y) = g(x, y) / b(x, y) = \exp(-j\phi(x, y))$. From $h(x, y)$, the photo-thermal phase shift at any point can be determined by:

$$\Delta\phi(x, y) = \arctan \left[\frac{\text{Im}\{h(x, y)\}}{\text{Re}\{h(x, y)\}} \right]. \quad (8)$$

Evaluating this expression around the optical propagating axis, one can calculate the phase difference given by Eq. (4) and estimate the 2PA coefficient of the medium.

3. Experimental details and results

The TL technique, based on a Rayleigh interferometer, used the experimental geometry shown in Fig. 2. A mode-locked Coherent Mira 900 laser system was used, delivering 200 fs pulses at 76 MHz repetition rate, tunable from 700 to 1000 nm. The fs laser beam was split into two beams; the transmitted probe beam and reflected pump beam. The radius of the probe beam was increased by a factor of ca. ten in order to illuminate two pinholes of 0.5 mm in diameter each with 3 mm of separation from their centers. The probe and reference beams,

after passing through a 1 mm of path length quartz cell, were combined by lens 2 ($f = 20\text{ cm}$ and $D = 4\text{ cm}$), forming a parallel interference pattern in its focal plane. In this modified Rayleigh interferometer, the typical optical delay line was not necessary to adjust the path difference between the two interferometer branches because the system compensated the optical path differences between beams <1> and <2>, improving the contrast between fringes.

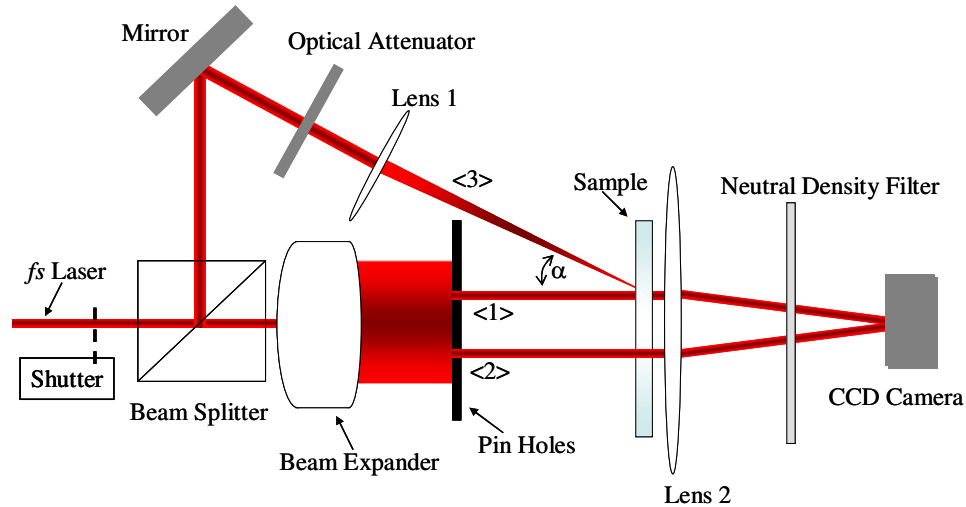


Fig. 2. Top-view of the experimental setup, the laser polarization is perpendicular to the plane of the figure. A neutral density filter wheel serves as the optical attenuator.

To observe and record the interferograms, a CCD camera was used with resolution of 640 x 480 pixels and 255 gray levels. Neutral density filters, placed in front of the camera, allowed an appropriate intensity level of the interferogram. The reflected pump beam (<3>) was focused into the sample by means of lens 1, adjusting the power with an optical attenuator. The focal length of lens 1 was adjusted in order to increase or decrease the beam waist into the sample. This radius was measured by forming its image on a calibrated CCD camera. The angle α between beams <1> and <3> was set to be small enough in order to consider that both beams are coaxial with respect to the optical axis; variation of the optical path length of the pump beam into the sample induced by this angle was also neglected. To control the sample exposure to the pump beam, a high-speed shutter was used with an exposure time of one second.

During the experiment, a movie of one-second duration was recorded. From this, the first and the last frames were extracted and processed by using typical Fourier's analysis. The first frame, linear interferogram, only carried the linear phase shift produced by beams <1> and <2>; it was assumed that the photo-thermal phase shift produced by the heat accumulation in the sample at this time could be neglected. The phase shift of this interferogram with respect to the one recorded in absence of the pump beam was compared, with no observed photo-thermal phase shift. In this case, the comparison of intensity profile interferograms did not show any change between their phases. The last frame, nonlinear interferogram, contained the nonlinear interference pattern induced by the photo-thermal effect accumulated during the 1 s time period.

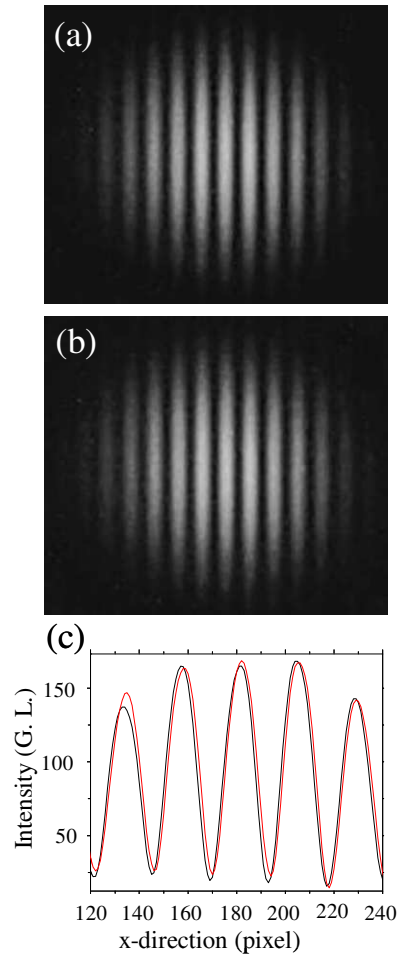


Fig. 3. Experimental interferograms: (a) linear interferogram at the initial state of the photo-thermal process, (b) nonlinear interferogram, and (c) intensity profile interferograms obtained from experimental images. The red fringes in (c) show the phase shift when the thermal lens is induced. Intensity is expressed by Gray level units (G.L.).

To test this method, a sample of CS_2 of 1 mm of path length was used, which is well known for its high nonlinear optical properties [2,16,17]. Figures 3a and 3b show typical experimental interferograms obtained at $\lambda = 800\text{nm}$, with Fig. 3b representing the nonlinear interferogram. The two pinhole interferometer system provided a high spatial quality of the reference and probe beam, confirmed by the good contrast observed in the interferograms. As a consequence, the statistical uncertainty of the measurements was reduced. Any contribution of the flatness of the cell walls was not considered in the nonlinear phase shift.

Figure 3c shows the intensity profiles determined from the middle of each image in the horizontal direction (x-direction). As can be seen, the phase is weakly shifted to the right side (red line) when the stationary thermal lens is induced; demonstrating that the fringe displacement does not produce any effect in the carrier frequency of the interference pattern, only the phase is affected.

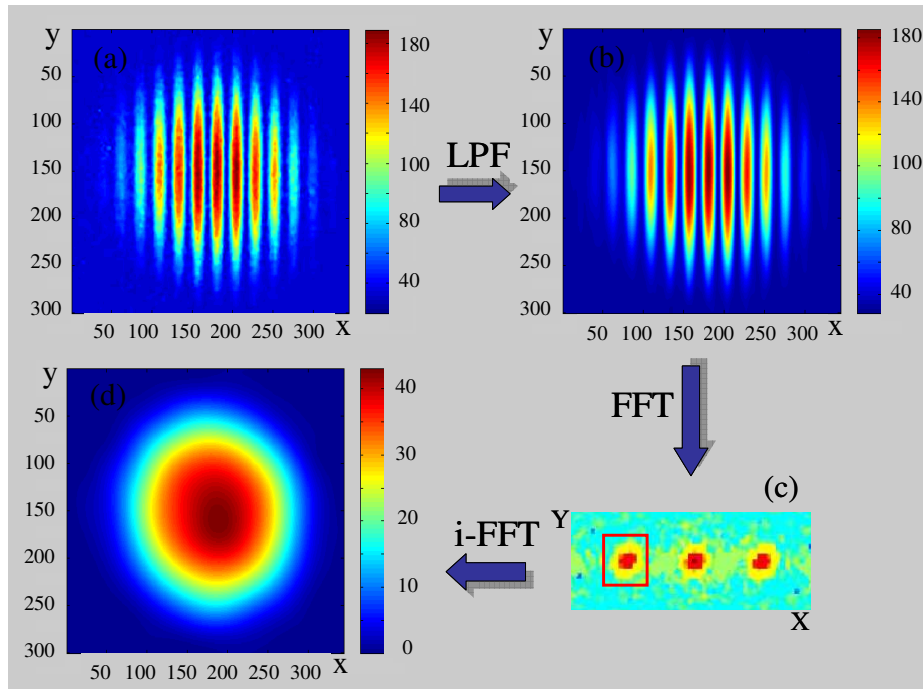


Fig. 4. Summary of the steps used in the Fourier analysis for CS2. (a) Experimental nonlinear interferogram. (b) Filtered interference pattern. (c) Fourier space showing the Dirac's distributions. (d) Isolated probe beam distribution carrying the photo-thermal phase shift.

The images were processed using standard image processing techniques [18]. In Fig. 4, the steps applied during the processing of the nonlinear interference pattern are summarized; the same Fourier treatment was performed on the linear interferogram in order to obtain the function $b(x, y)$. From the experimental interference pattern (a), only the high frequency components and noise were removed by using a low pass Fourier filter (LPF), the carrier frequency and the intensity levels of the interferogram remained constants (see Fig. 4b). The 2D Fast Fourier Transform (FFT) was applied to the filtered pattern and its nonlinear spatial spectrum can be observed in Fig. 4c, where the three terms of Eq. (6) are represented in this image as three distinct Dirac's spots. The red square frame in Fig. 4c indicates the signal selected by the band pass filter (the Dirac's distribution) that contains the photo-thermal phase shift. This filter was implemented in the software, and it basically consisted in cropping the selected spot from the image. This distribution was again transformed by using an inverse 2-D FFT algorithm to obtain the complex function Eq. (7), shown in Fig. 4d.

After the Fourier analysis was conducted for both interference patterns, Eq. (7) was used to extract the photo-thermal phase shift induced by the HRR laser. The resulting phase shift map is shown in Fig. 5. The absorption coefficient β was estimated using this figure and Eq. (4). The red square centered in the middle of the map indicates the area where the photo-thermal phase shift around the optical axis was evaluated. This area contains 36 points, allowing one to calculate an average value of the magnitude of the phase difference given by Eq. (4).

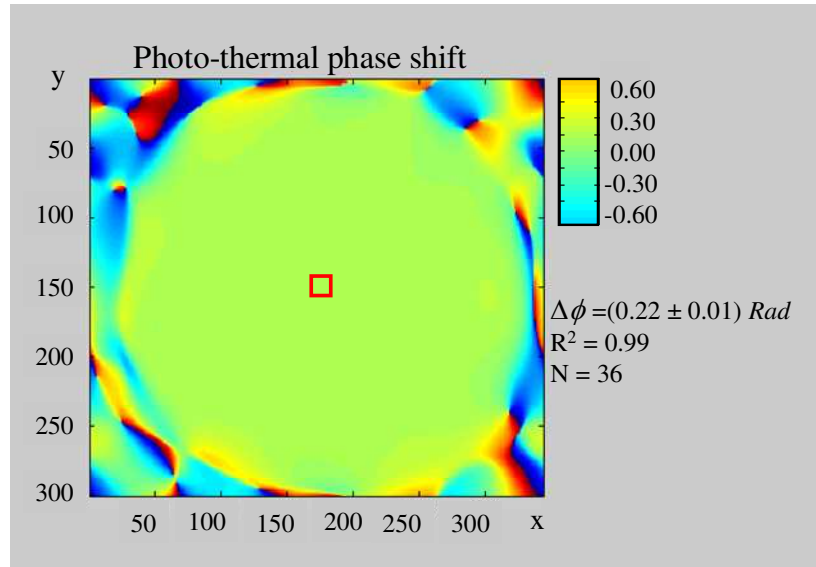


Fig. 5. Photo-thermal phase map extracted from interferograms shown in Figs. 3a and 3b. The red square indicates the area where the phase difference was evaluated.

By using the phase magnitude ($\phi_0 = 0.22$) and the parameters given in Table 1 for CS_2 in the Eq. (4), $\beta = (5.6 \pm 0.2) \times 10^{-13} \text{ m/W}$ was obtained for the 2PA coefficient of CS_2 , in good agreement with that previously reported by Ganeev *et al.* ($4.2 \times 10^{-13} \text{ m/W}$) [16] and Couris *et al.* (ca. 10^{-13} m/W) [17]. The indicated error was estimated from the relative error of the phase difference, from the fluctuations in the power and wavelength of the laser, and from the error of the estimation of the size of the pump beam radius. To ensure the 2PA process was indeed operative in our measurements, the behavior of the photo-thermal phase shift was determined at different incident powers. Figure 6a shows the log-log plot of the experimental measurements obtained for the CS_2 at 800 nm; the calculated slope indicates a quadratic dependence between the phase shift and the incident power, verifying our model.

Table 1. Parameters of the four samples.

Material	κ ($\text{Wm}^{-1}\text{K}^{-1}$)	dn/dT (K^{-1}) 10^{-4}	w (μm)	P (W)	Φ -	$\langle \lambda_e \rangle$ (nm)	[C] (M) 10^{-4}
CS_2	0.161	5.00	6	0.24	0.00	-	-
RhB	0.200	3.94	37	0.15	0.70	583	1.0
Rh6G	0.200	3.94	37	0.16	0.95	572	2.5
Fluorescein	0.598	0.91	6	0.35	0.90	545	1.9

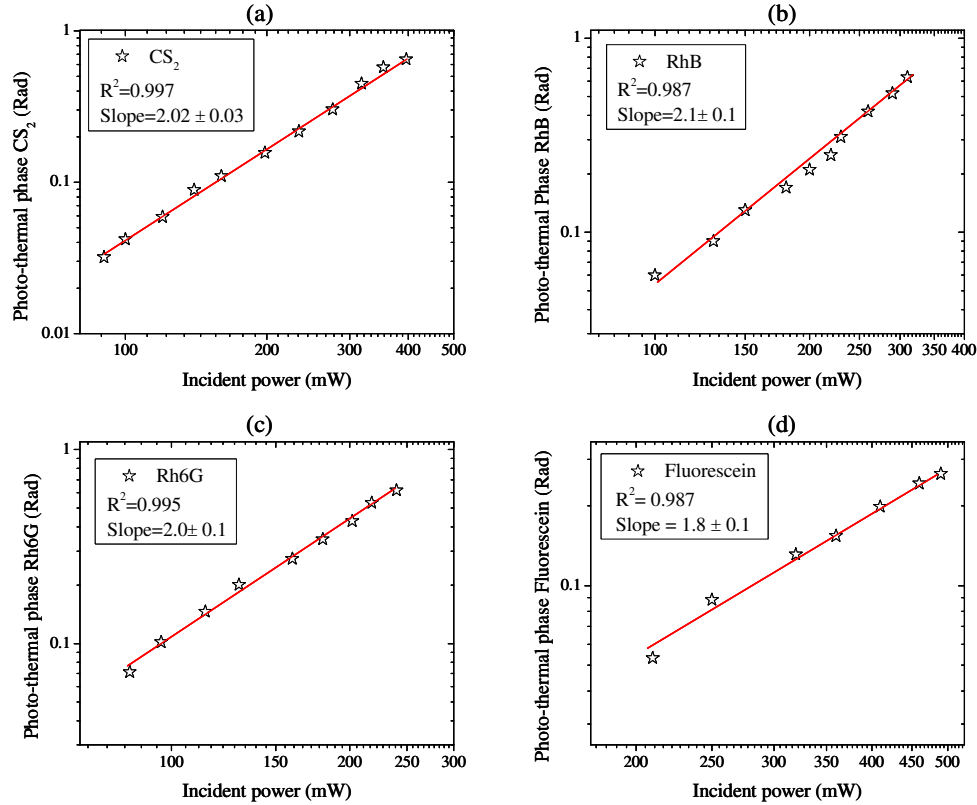


Fig. 6. Log-Log plots for all tested samples. The red straight lines indicate the best fit obtained by linear regression for each sample.

To estimate the resolution of our results, Eq. (4) is rewritten in the following simplified form: $\Delta\varphi = \left[\left(\frac{dn}{dT} \right) P / \lambda \kappa \right] q$, where $q = \beta L I_0$ is the nonlinear absorbance and I_0 is the on-axis intensity at the radius beam w . Analogous to the one-photon case [8], in our approach we define the accumulative enhancement factor (terms enclosed in the squared brackets) with respect to a nonlinear transmission technique [2,3]. The minimum phase difference measurable with our experimental setup is 0.03 Rad , and from Fig. 6a, this limit is approximately reached at 90 mW of incident power. This was measured by varying the incident power of the pump beam (as shown in Fig. 6a) and recording the interferograms. Taking the values for $\kappa = 0.161 \text{ Wm}^{-1} \text{ K}^{-1}$, $\left(\frac{dn}{dT} \right) = 5 \times 10^{-4} \text{ K}^{-1}$ and $\lambda = 800 \text{ nm}$, the enhancement factor is about 10^4 . Consequently, taking into account these values for the enhancement factor and the measurable phase difference, we calculated that the minimum nonlinear absorbance, q , detectable with our system is as low as 10^{-6} , a value difficult or impossible to detect using the classical nonlinear transmittance technique [1–3]. In addition to the typical sensitivity of the TL technique in detecting low absorbances [7–9], the Rayleigh interferometer can measure, with high accuracy, weak refractive index changes [13], further improving the sensitivity of our system.

Two-photon absorption coefficients can be also expressed in term of the 2PA cross section δ by means of $\beta = 2[C]N_A\delta/h\nu$, where N_A is the Avogadro's number, $[C]$ is the concentration of the sample, h is Planck's constant, and ν is the frequency of the excitation light. By considering this relation and Eq. (4), when fluorescence occurs in addition to the

photo-thermal effect, it is possible to calculate the absolute values of δ for fluorescent molecules in solution. We tested this interesting application with standard organic dye molecules, such as Rhodamine B (RhB), Rhodamine 6G (Rh6G), and Fluorescein. The experimental results are shown in Figs. 6b, 6c, and 6d, for excitation of each molecule at 800 nm, demonstrating that the phase difference varied quadratically with the incident power for RhB and Rh6G. This indicated that the extracted phase difference from the interferograms was produced by the 2PA process.

From the experimental data plotted in Fig. 6b, the absolute values of δ for RhB were estimated. Taking the photo-thermal phase shift as 0.14 Rad along with the parameters given in Table 1, we obtain $\delta_{RhB} = (105 \pm 2) \text{ GM}$. Although this value is smaller than that measured by the fluorescence method, Xu and Webb (ca. 140 GM) [4] and Makarov *et al.* (ca. 120 GM) [6], it is within experimental error of the cited values. We estimated the excitation intensity required for our system to induce the 2PA process in RhB at 800 nm was about $10^{30} \text{ photons.cm}^2.\text{s}^{-1}$. Although this is approximately one order of magnitude larger than that frequently used in fluorescence methods [4], this intensity level is weak enough as not to be concerned with any spurious effects occurring during measurement. The same experimental parameters were used to measure δ for Rh6G. In this case, the measured phase shift from Fig. 6c was 0.22 Rad and $\delta_{Rh6G} = (61 \pm 1) \text{ GM}$, very close to previously reported value by Makarov *et al.* (65 GM) [6].

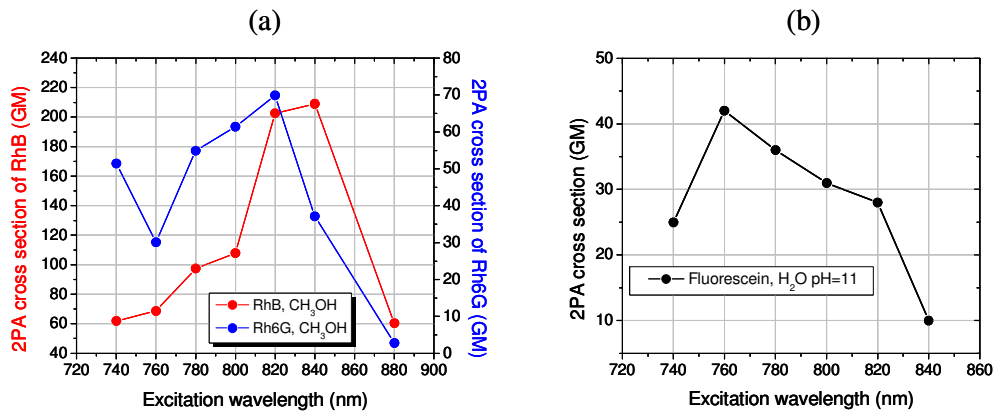


Fig. 7. Two-photon absorption spectra for the fluorescent molecules studied. RhB and Rh6G were prepared in methanol solution, while the Fluorescein was evaluated in alkaline water.

Although a small deviation from the second order dependence was observed for the Fluorescein sample (see Fig. 6c), our estimation of δ ($(31 \pm 1) \text{ GM}$ at $\Delta\phi = 0.14 \text{ Rad}$ and $P = 350 \text{ mW}$) yielded a result comparable with those separately published by Makarov *et al.* (36 GM) [6], and Albota *et al.* (36 GM) [19]. A possible reason for this discrepancy was due to the high intensity level applied to this sample ($I_0 \approx 6 \text{ GW/m}^2$); excited-state saturation could induce this deviation from quadratic dependence. Figure 7 illustrates the absolute 2PA cross section spectra measured at different excitation wavelengths for the three dyes tested in solution.

Finally, this method was evaluated to make relative measurements. This consisted of estimating the 2PA cross section ratio between two different samples; the reference and test samples. Since the beam waist is wavelength dependent, this measurement eliminates its influence on the estimation of δ . We performed the measurements using a pump beam that was strongly focused in the sample and considered the following expression:

$$\frac{\delta_s}{\delta_r} = \left(\frac{\Delta\phi_s}{\Delta\phi_r} m \right), \quad (9a)$$

$$m = \frac{[C_s] P_r^2 \left[\kappa_s (dn_r/dT) \right] \left(\frac{1 - \Phi_r \lambda / 2 \langle \lambda_e \rangle_r}{1 - \Phi_s \lambda / 2 \langle \lambda_e \rangle_s} \right)}{[C_s] P_s^2 \left[\kappa_r (dn_s/dT) \right]}. \quad (9b)$$

where subscripts s and r indicate sample and reference, respectively. We used the δ values of RhB reported in [6] as reference. The nonlinear absorption values indicated in Table 2 for Rh6G and Fluorescein were consistent with the ones reported above and close to those reported in the literature [6,19], showing the simplicity and precision of the relative measurements. In addition, Table 2 lists the ratio of the 2PA absorption cross section of the sample and reference, measured under identical conditions.

Table 2. Relative δ values obtained from Rh6G and Fluorescein solutions. The reference 2PA cross sections values for RhB are from reference 6.

$\lambda_{\text{excitation}}$ (nm)	Rh6G		Fluorescein	
	780	800	780	800
$\delta_{\text{sample}} / \delta_{\text{RhB}}$	0.562	0.518	0.504	0.321
δ_{RhB} (GM) ^a	95	120	95	120
δ_{sample} (GM)	53	62	48	39

^aFrom Opt. Express **16**, 4029 (2008).

4. Conclusion

A method was developed that allows fast and accurate measurements of the 2PA cross sections in liquid samples using two readily obtained images. This method relies on determination of the phase shift of an interference pattern induced by an accumulative thermal lens effect in a liquid sample. The technique was validated by measuring 2PA coefficients of standard nonlinear media CS₂ (neat) and the 2PA cross section of widely used organic molecule standards (Rhodamine B, Rhodamine 6G, and Fluorescein), providing results that were in good agreement with those previously reported in the literature. Since the experimental data can be acquired rapidly, this technique may be useful to determine 2PA coefficients for samples susceptible to photodegradation, such as photoinitiators, reagents for photouncaging, and photosensitizers. The results obtained using the accumulative photo-thermal effect and Rayleigh interferometry demonstrate that this new technique is robust, sensitive, and has the accuracy to measure 2PA cross sections in dilute solutions.

Acknowledgments

We wish to acknowledge the National Science Foundation (ECS-0621715 and CHE-0832622) for support of this work.